

BEHAVIOR OF FIBER REINFORCED POLYMER GROUTED SPLICE  
CONNECTIONS

KIARASH KOUSHFAR

A thesis submitted in fulfillment of the  
requirements for the award of the degree of  
Doctor of Philosophy (Civil Engineering)

School of Civil Engineering  
Faculty of Engineering  
Universiti Teknologi Malaysia

JUNE 2020

## DEDICATION

This thesis is dedicated to my beloved father, Abbas Koushfar who taught me that the best kind of knowledge to have is that which is learned for its own sake. It is also dedicated to my beloved mother, Fatemeh Razavi who taught me that even the largest task can be accomplished if it is done one step at a time. This thesis is dedicated to my dearest brothers, Kia and Keyarmin Koushfar.

Also, this thesis is dedicated to all those who believe in the richness of learning.

## ACKNOWLEDGEMENT

The realization of this research was only possible due to the several people's collaboration, to which desire to express my gratefulness.

I would like to thank my supervisors, Prof. Dr. Ahmad Baharuddin Abd. Rahman, Associate Prof. Dr. Yusof Ahmad and Dr. Sophia C. Alih. I am grateful for the trust deposited in my work and for the motivation demonstrated along this research. Their support was without a doubt crucial in my dedication this investigation. Prof. Dr. Ahmad Baharuddin Abd. Rahman has been the ideal thesis supervisor. Without his inspirational instruction and guidance I was not able to complete this project. His sage advice, insightful criticisms, and patient encouragement aided the writing of this thesis in innumerable ways.

Gratitude is also expressed to my co-supervisor whom without his support this project would not have been possible. Associate Prof. Dr. Yusof Ahmad and Dr. Sophia C. Alih for providing the materials which immensely eased my financial burden. His guidance, support, understanding, and patience throughout my research was greatly needed and deeply appreciated.

Appreciation is extended to all laboratory staff for advices and suggestions of the work, and for the friendship that always demonstrated along these months of this project.

## ABSTRACT

Grouted splice connections are widely used in joining precast concrete wall-to-wall and wall-to-column connections. However, not many studies on grouted splice connections could identify and predict their minimum bar embedded lengths and ultimate strength precisely which may lead to catastrophic failures in the structure. Moreover, the majority of the published studies are limited to conventional steel products which could not predict satisfactorily the behavior and performance of the grouted splice connections particularly when new materials and methods are adopted. In this regard, the main aim of this study was to investigate the behavior and performance of grouted splice connections using sleeves manufactured with steel pipes and new sheet materials of Carbon Fiber Reinforced Polymer (CFRP) and Glass Fiber Reinforced Polymer (GFRP) sleeves. In order to predict the behavior and performance of the proposed FRP grouted splice connections, empirical relationships, Artificial Neural Network (ANN), and Finite Element Method (FEM) were developed. In Phase 1 of this study, a total of 165 grouted splice connections with different shapes, diameters, embedded lengths, and sleeve materials were tested to failure under incremental tensile load. In Phases 2 and 3, the experimental results obtained from Phase 1 were used as raw data to establish the analytical behavior and performance of the grouted sleeve connections using ANN and FEM, respectively. The results of Phase 1 show that the CFRP sleeves provided better confinement effect, hence contributed higher bond and tensile strengths compared to GFRP sleeves with similar design parameters. New equations were developed based on experimental results in Phase 1 and had shown good prediction of the ultimate tensile strengths of the proposed connections with the reliability ratios close to 1.0. Then in Phase 2, the analytical results demonstrate the superiority of ANN model compared to the other methods in predicting the ultimate tensile strength and behavior of all the proposed connections. The advantage of ANN model is the minimum reliance on the experimental data in estimating the performance of the specimens. The FEM results of Phase 3 indicate that the predicted behaviors of the grouted splices are in line with the experimental results. Also, the FEM results show the importance of providing adequate confinement at regions near the center of the sleeve where the highest stress concentration occurs. In conclusion, CFRP sheets generated the highest confinement, while the embedment length, interlocking mechanism and shape of the FRP sleeves contributed the highest impact on the bond strength, axial stiffness, ultimate tensile strength and ductility of the proposed FRP specimens. Finally, although the proposed empirical relationships predicted acceptable ultimate tensile strength of FRP specimens with high accuracy, the ANN model found to be more superior and it can be used with minimum dependency on experimental data.

## ABSTRAK

Sambungan sambat berturap digunakan secara meluas bagi menyambungkan konkrit pratuang dinding-ke-dinding dan dinding-ke-tiang. Bagaimanapun, tidak banyak kajian mengenai sambungan sambat dapat mengenal pasti dan meramalkan minimum panjang tambatan dan kekuatan tegangan muktamad dengan tepat yang boleh menyebabkan kegagalan bencana dalam struktur. Lebih-lebih lagi, sebahagian besar kajian yang diterbitkan hanya terhad kepada produk keluli konvensional dapat tidak meramalkan tingkah laku dan prestasi dengan memuaskan terutamanya apabila bahan dan kaedah baru digunakan. Dalam hal ini, objektif utama kajian ini adalah untuk mengkaji tingkah laku dan prestasi sambungan sambat berturap menggunakan selongsong daripada paip keluli dan bahan kepingan baru Karbon Tetulang Gentian Kaca (CFRP) dan Polimer Tetulang Gentian Kaca (GFRP). Untuk meramalkan tingkah laku dan prestasi sambungan FRP yang dicadangkan hubungan empirical, Rangkaian Neural Buatan (ANN) dan Unsur Terhingga (FEM) telah dibangunkan. Dalam kajian Fasa 1, sejumlah 165 sambungan sambat berturap dengan bentuk, diameter, dan selongsong bahan yang berbeza telah diuji sehingga gagal di bawah beban tegangan bertambah untuk menyiasat kelakuan dan prestasi sambungan. Dalam Fasa 2 dan 3, keputusan ujikaji yang diperolehi dari Fasa 1 telah digunakan sebagai data mentah untuk menentukan kelakuan analitikal dan prestasi sambungan selongsong menggunakan kaedah ANN dan FEM. Keputusan kajian Fasa 1 menunjukkan selongsong CFRP memberikan kesan pengurangan lebih baik, serta menghasilkan kekuatan ikatan dan kekuatan tegangan yang lebih tinggi berbanding GFRP bagi konfigurasi yang sama. sambat lain. Persamaan baru juga telah dibangunkan berdasarkan keputusan ujikaji Fasa 1 dan telah menunjukkan ramalan yang baik dalam menentukan kekuatan tegangan muktamad bagi sambungan yang dicadangkan dengan nisbah kebolehpercayaan menghampiri 1.0. Kemudian dalam Fasa 2, hasil analitikal menunjukkan keunggulan model ANN berbanding kaedah lain dalam meramalkan kekuatan tegangan muktamad dan tingkah laku semua sambungan yang dicadangkan. Kelebihan model ANN adalah pergantungan minima data ujikaji dalam menganggarkan prestasi sambungan. Keputusan FEM bagi kajian Fasa 3 pula menunjukkan tingkah laku yang diramalkan FEM adalah sejajar dengan keputusan ujikaji. Selain itu, keputusan FEM menunjukkan kepentingan menyediakan pengurangan yang mencukupi di kawasan pertengahan selongsong di mana penumpuan tegasan tertinggi berlaku. Kesimpulannya, lembaran CFRP memberikan pengurangan tertinggi, manakala panjang tambatan, mekanisme saling mengunci dan bentuk sambungan FRP menyumbang kesan tertinggi pada kekuatan ikatan, kekukuhan paksi, kekuatan tegangan muktamad dan kemuluran spesimen FRP yang dicadangkan. Akhirnya, walaupun hubungan empirikal yang dicadangkan meramalkan kekuatan tegangan muktamad mutlak spesimen FRP dengan ketepatan yang tinggi, model ANN didapati lebih unggul dan dapat digunakan dengan pergantungan minimum pada data eksperimen.

## TABLE OF CONTENT

	<b>TITLE</b>	<b>PAGE</b>
	<b>DECLARATION</b>	<b>ii</b>
	<b>DEDICATION</b>	<b>iii</b>
	<b>ACKNOWLEDGEMENT</b>	<b>iv</b>
	<b>ABSTRACT</b>	<b>v</b>
	<b>ABSTRAK</b>	<b>vi</b>
	<b>TABLE OF CONTENTS</b>	<b>vii</b>
	<b>LIST OF TABLES</b>	<b>xiii</b>
	<b>LIST OF FIGURES</b>	<b>xvi</b>
	<b>LIST OF ABBREVIATIONS</b>	<b>xxv</b>
	<b>LIST OF SYMBOLS</b>	<b>xxvi</b>
	<b>LIST OF APPENDICES</b>	<b>xxix</b>
<b>CHAPTER 1</b>	<b>INTRODUCTION</b>	<b>1</b>
1.1	Introduction	1
1.2	Problem Statement	4
1.3	Objectives	6
1.4	Scopes of Research	6
1.5	Thesis Outline	7
<b>CHAPTER 2</b>	<b>LITERATURE REVIEW</b>	<b>9</b>
2.1	Introduction	9
2.2	Bond Mechanism	10
2.2.1	Chemical Adhesion	13
2.2.2	Frictional Resistance	14
2.3	Factors Influencing Bond Behavior	15
2.3.1	Confinement	15
2.3.2	Strength of Bonding Material	22
2.4	Bond between Fiber-Aluminum Interfaces	24
2.5	Previous Studies of Mechanical Splices	31

2.6	Experimental Setups for Tensile Load Test	65
2.7	Summary	67
<b>CHAPTER 3 RESEARCH METHODOLOGY</b>		<b>69</b>
3.1	Introduction	69
3.2	Test Specimens	73
3.2.1	Labeling of Specimens	77
3.2.2	Control Specimens	79
3.2.3	Rigid Corrugated Aluminum Sleeve Wrapped with FRP Sheets (R-FRP)	83
3.2.4	Flexible Corrugated Aluminum Sleeve Wrapped with FRP Sheets (F-FRP)	84
3.2.5	Tapered GFRP Grouted Splices (T-FRP)	86
3.3	Preparation of Grouted Splices	88
3.3.1	Preparation of R-FRP and F-FRP Sleeves	88
3.3.2	Preparation of T-FRP Sleeves	89
3.3.3	Preparation of Bolted and Welded Sleeves	90
3.3.4	Installation and Preparation of Grouted Splices	90
3.4	Materials Properties	93
3.4.1	Sika Grout-215	93
3.4.2	Reinforcement Bars	94
3.4.3	Epoxy Resin, Epicote 1006	95
3.4.4	Glass Fibers	96
3.4.5	Carbon Fibers	97
3.5	Outline of the Tensile Test Program of the Grouted Splices	98
3.6	Tensile Test of FRP Composite Materials	100
<b>CHAPTER 4 BEHAVIOR OF THE GROUDED SPLICES UNDER INCREMENTAL TENSILE LOAD</b>		<b>103</b>
4.1	Introduction	103
4.2	Test Results of Tensile Load Test	103
4.2.1	Ultimate Tensile Strengths of Grouted Splices	110
4.2.2	Measurement of Ultimate Displacement of Grouted Splices	113

4.2.3	Failure Modes of Grouted Splices	114
4.3	Load-Displacement Responses of Grouted Splices	115
4.4	Behavior of Strain of Grouted Splice Components	118
4.4.1	Tensile Strain Responses in Spliced Bar	118
4.4.2	Tensile Strain Responses in FRP Sleeve	120
4.4.3	Transverse Strain Responses in FRP Sleeve	122
4.5	Mechanisms and Modes of Failure of Grouted Splices	124
4.5.1	Grout Bond-Slip Failure	125
4.5.2	Bar Bond-Slip Failure	126
4.5.3	Aluminum Tube bond-slip Failure	128
4.5.4	Sleeve Fracture	129
4.5.5	Bar Fracture	131
4.6	Yield Point and Stiffness of Grouted Splices	132
4.7	Ratios of Strength, Ductility and Yield of Grouted Splices	145
4.8	Bond Stress in Grouted Splices	153
4.9	The Bar-Grout and Sleeve-Grout Interlocking Mechanisms and the Confinement Effects on the Load Resisting Mechanisms of the Grouted Splices	155
4.10	Effects of Sleeve Design parameters on Tensile Strength of the Grouted Splices	158
4.11	Effects of Sleeve Diameter on Tensile Strength, Pre-Yield Stiffness, and Bond Strength	164
4.12	Effects of Bar Embedded Length on Tensile Strength and Pre-Yield Stiffness of the FRP Grouted Splices	166
4.13	Minimum Bar Embedded Length	169
4.13.1	Determining the Minimum Bar Embedded Length Using Graphical Method	170
4.13.2	Determining the Minimum Bar Embedded Length Using Ultimate Bond Stress Method	175
4.14	Prediction of Tensile Strength of FRP Grouted Splice Connections	177
4.15	Summary	186
 <b>CHAPTER 5 PREDICTING THE BEHAVIOR OF THE FRP GROUTED SPLICE CONNECTION USING ARTIFICIAL NEURAL NETWORKS</b>		<b>189</b>
5.1	Introduction	189



5.2	Network Architectures	190
5.3	Neural Network Modeling	192
5.4	Comparison of ANN Strength Model and Empirical Equations Derived by SPSS software with Experimental Results	199
5.5	Estimating the Tensile Strength of the Grouted Splices with the Proposed Minimum Bar Embedded Lengths	208
5.6	Comparison between ANN Model and Analytical Expression of the Load-Displacement Behavior of FRP Grouted Splice Connections	215
5.7	Comparison of ANN Strength Model with Empirical Models	218
5.8	Summary	229
 <b>CHAPTER 6 FINITE ELEMENT MODEL</b>		 <b>231</b>
6.1	Numerical Modeling	231
6.2	Steps in Finite Element Analysis	232
6.2.1	Pre-Processing	232
6.2.2	Processing	233
6.2.3	Post-Processing	233
6.3	General Analysis Procedure for Static Structural Problems	234
6.3.1	Build the Simulation Model	235
6.3.1.1	Clear the Database	235
6.3.1.2	Attribute Suitable Material Properties to the Model	235
6.3.1.2.1	Grout Material	236
6.3.1.2.1.1	Description of PLANE182 Element	236
6.3.1.2.1.2	Description of PLANE183 Element	237
6.3.1.2.2	FRP Materials	240
6.3.1.2.3	Aluminum Tube	241
6.3.1.2.4	Steel Reinforcement Material	242
6.3.1.3	Developing the Geometric Model of the Problem	245
6.3.1.3.1	Solid Modeling	246
6.3.1.3.2	Direct Generation	247
6.3.1.3.3	Importing External CAD	248

	Geometry	248
6.3.1.4	Defining the Contact Elements	249
6.3.1.4.1	CONTA171 2-D Surface-to-Surface Contact	249
6.3.1.4.2	CONTA172 2-D 3-Node Surface-to-Surface Contact	250
6.3.1.5	Mesh the Model	252
6.3.1.6	Impose the Boundary and Loading Conditions	253
6.3.1.7	ANSYS® Solution Control	255
6.3.1.7.1	The Full Method	256
6.3.1.7.2	The Reduced Method	256
6.3.1.7.3	The Mode Superposition Method	257
<b>CHAPTER 7</b>	<b>PREDICTING THE BEHAVIOR OF THE FRP GROUDED CONNECTIONS USING FINITE ELEMENT ANALYSIS</b>	<b>259</b>
7.1	Introduction	259
7.2	Test Results of Finite Element Analysis of the Grouted Splices	260
7.3	Comparison of Load-Displacement Responses between FE Analysis and Experimental Results of Rigid Corrugated Aluminum Tube Wrapped with FRP Sheets (R-FRP)	260
7.4	Comparison of Load-Displacement Responses between FE Analysis and Experimental Results of Flexible Corrugated Aluminum Tube Wrapped with FRP Sheets (F-FRP)	263
7.5	Comparison of Load-Displacement Responses between FE Analysis and Experimental Results of Bolted and Welded Steel Grouted Splices (K-W)	266
7.6	Finite Element Stresses Distribution Contours of the Grouted Splices	268
7.7	Summary	276
<b>CHAPTER 8</b>	<b>CONCLUSIONS</b>	<b>279</b>
8.1	Introduction	279
8.2	Conclusion	280
8.2.1	Performance and Behavior of the Proposed Grouted Splice Connections Under Incremental Tensile Load	280

8.2.2	Analytical Prediction of the Ultimate Tensile Strength, Load-Displacement Behavior, and Minimum Embedded Length of FRP Grouted Splice Connections	281
8.2.3	Predicting the Behavior and Performance of The FRP Grouted Splices Using Neural Networks	283
8.2.4	Behavior of the Grouted Splice Connections Using Finite Element Analysis (FEA)	284
8.3	Future Works	285

<b>REFERENCES</b>	<b>287</b>
-------------------	------------

## LIST OF TABLES

<b>TABLE NO.</b>	<b>TITLE</b>	<b>PAGE</b>
Table 2.1	The interlaminar shear strength of Novel FML and Glare laminate [85]	30
Table 3.1	Examples of labeling of specimens	79
Table 3.2	Geometrical properties of control specimens, K-P series	80
Table 3.3	Geometrical properties of control specimens, K-W series	81
Table 3.4	Geometrical properties of control specimens, K-R series	82
Table 3.5	Geometrical properties of control specimens, K-F series	82
Table 3.6	Geometrical properties of R-FRP series	84
Table 3.7	Geometrical properties of F-FRP series	85
Table 3.8	Geometrical properties of T-FRP series	87
Table 3.9	Mechanical and Physical Properties of Sika Grout-215	94
Table 3.10	Properties of Y16 reinforcement bars under incremental tensile load	95
Table 3.11	Mechanical and Physical Properties of EPICOTE 1006 SYSTEM	96
Table 3.12	Specification of woven roving E-glass fibers	97
Table 3.13	Specification of woven roving E-glass fibers	98
Table 3.14	Geometrical properties of FRP composite coupons	102
Table 4.1	Results of tensile load tests of control series	104
Table 4.2	Results of tensile load tests for R-FRP grouted splices	105
Table 4.3	Results of tensile load tests for F-FRP grouted splices	107
Table 4.4	Results of tensile load tests for T-FRP grouted splices	108
Table 4.5	Tensile Strength, $\bar{P}_u$ , of R-FRP and F-FRP grouted splices	111
Table 4.6	Tensile Strength, $\bar{P}_u$ , of T-FRP grouted splices	112
Table 4.7	Pre-yield stiffness and yield point of control and R-FRP series	139
Table 4.8	Pre-yield stiffness and yield point of F-FRP series	140
Table 4.9	Pre-yield stiffness and yield point of T-FRP series	142
Table 4.10	Pre-yield stiffness of R-FRP and F-FRP series	144
Table 4.11	Pre-yield stiffness of T-FRP series	144

Table 4.12	The yield, strength, and ductility ratios of R-FRP series	146
Table 4.13	The yield, strength, and ductility ratios of R-FRP series	148
Table 4.14	The yield, strength, and ductility ratios of T-FRP grouted splices	149
Table 4.15	Strength ratio, $\bar{\mu}_s$ , of R-FRP and F-FRP grouted splices	152
Table 4.16	Strength ratio, $\bar{\mu}_s$ , of T-FRP grouted splices	153
Table 4.17	Bond stress, $\bar{\tau}$ , of R-FRP and F-FRP grouted splices	154
Table 4.18	Bond stress, $\bar{\tau}$ , of T-FRP grouted splices	155
Table 4.19	Minimum bar embedded length, $l_{min,gr}$ , of R-FRP and F-FRP specimens	174
Table 4.20	Minimum bar embedded length, $l_{min,gr}$ , of T-FRP specimens	174
Table 4.21	Minimum bar embedded length, $l_{min,ult}$ , of R-FRP and F-FRP specimens	176
Table 4.22	Minimum bar embedded length, $l_{min,ult}$ , of T-FRP specimens	176
Table 4.23	Comparisons between ultimate tensile strength of predicted using Eqn. 4.61 and experimental and of R-FRP and F-FRP grouted splices	183
Table 4.24	Comparisons between ultimate tensile strength of predicted using Eqn. 4.62 and experimental of T-FRP grouted splices	184
Table 5.1	Scaling equations for input and target nodes	194
Table 5.2	Distribution of differences for different strength models relative to experimental values	202
Table 5.3	Comparison between experimental tensile strength, $P_{u,Exp}$ , predicted tensile strength by neural networks, $P_{u,NN}$ , and predicted tensile strength by Equation 5.2, $P_{u,pre}$ , of the grouted splices	203
Table 5.4	Comparison between experimental tensile strength, $P_{u,Exp}$ , predicted tensile strength by neural networks, $P_{u,NN}$ , and predicted tensile strength by Equation 5.3, $P_{u,pre}$ , of the grouted splices	204
Table 5.5	Comparison between experimental tensile strength, $P_{u,Exp}$ , predicted tensile strength by neural networks, $P_{u,NN}$ , and predicted tensile strength by Equation 5.4, $P_{u,pre}$ , of the grouted splices	206
Table 5.6	Minimum bar embedded length, $l_{min,gr}$ , and the relative tensile strengths of R-FRP and F-FRP specimens predicted by neural networks, $P_{u,NN}$	214

Table 5.7	Minimum bar embedded length, $l_{min,gr}$ , and the relative tensile strengths of T-FRP specimens predicted by neural networks, $P_{u,NN}$	214
Table 5.8	Comparison between experimental load-displacement behavior of specimen R-C7L125-1, $P_{Exp}$ , with the predicted behavior by neural networks, $P_{NN}$ , and Equations 5.5 and 5.6, $P_{pre}$	221
Table 5.9	Comparison between experimental load-displacement behavior of specimen F-G7L175-1, $P_{Exp}$ , with the predicted behavior by neural networks, $P_{NN}$ , and Equations 5.7 and 5.8, $P_{pre}$	224
Table 5.10	Comparison between experimental load-displacement behavior of specimen F-G7L75-1, $P_{Exp}$ , with the predicted behavior by neural networks, $P_{NN}$ , and Equations 5.9 and 5.10, $P_{pre}$	227
Table 6.1	Consistent unit systems	232
Table 7.1	Comparison between FE analysis tensile strength by ANSYS, $P_{u,FE}$ , and experimental tensile strength, $P_{u,Exp}$ , of R-FRP grouted splices	263
Table 7.2	Comparison between FE analysis tensile strength by ANSYS, $P_{u,FE}$ , and experimental tensile strength, $P_{u,Exp}$ , of F-FRP grouted splices	265
Table 7.3	Comparison between FE analysis tensile strength by ANSYS, $P_{u,FE}$ , and experimental tensile strength, $P_{u,Exp}$ , of K-W series	268

## LIST OF FIGURES

<b>FIGURE NO.</b>	<b>TITLE</b>	<b>PAGE</b>
Figure 1.1	Installation of grouted splice connections [6]	3
Figure 2.1	Procedure of installing grouted splice sleeve connections	10
Figure 2.2	Distribution of bond stress at different levels of load for short embedded lengths [25]	11
Figure 2.3	Bond stress versus slip response [32]	12
Figure 2.4	(a) Bond force transfer mechanisms [36] (b) Typical bond stress-slip relationship [38]	13
Figure 2.5	Development of concrete crushing in front of the rib as bar slips	14
Figure 2.6	Frictional model of bond; $f_b = \mu \cdot \sigma_{lat}$ [45]	16
Figure 2.7	Stress-slip responses under confinement of transverse reinforcement [44]	18
Figure 2.8	Relationships of $U/\sqrt{f_c}$ versus $\sqrt{f_n}$ by Untrauer [24]	19
Figure 2.9	Mechanism of bond resistance in confined concrete: (a) inclined cracks at steel lugs; (b) crushing and shear cracks of concrete keys; and (c) progressive shearing-off of the concrete keys [49]	21
Figure 2.10	Relationships of bond stress versus displacement [43]	23
Figure 2.11	Relationship of bond stress versus concrete strength [33]	24
Figure 2.12	Configuration of continuous fiber-metal-epoxy hybrid composite [73]	25
Figure 2.13	Tensile behavior of the laminates studied	26
Figure 2.14	Compressive behavior of the laminates studied	26
Figure 2.15	The stacking arrangement of the aluminum and composite sheets in the picture frame mold [80]	27
Figure 2.16	Typical load–displacement relationships of SCB tests at 2 mm/min on composites/untreated aluminum alloy 2024-T3 [80]	27
Figure 2.17	Summary of the interfacial fracture properties of aluminum-based system [80]	28
Figure 2.18	The mechanical tests: (a) tensile test; (b) flexural test; (c) interlaminar shear test; (d) floating roller peeling test [85]	29

Figure 2.19	The laminating design of novel FMLs [85]	29
Figure 2.20	The delamination of metal layer [85]	30
Figure 2.21	Mechanical connections	33
Figure 2.22	(a) and (b) Proprietary splices tested by Jansson, (c) test setup [11]	33
Figure 2.23	General features of HPWEM [112]	34
Figure 2.24	Sketch of proposed specimens by Qiong et al. [114]	35
Figure 2.25	Different types of grouted sleeve connections used by [114]	36
Figure 2.26	Details of the specimens used by Yajun et al. [115]	37
Figure 2.27	Grouted splice sleeve [109]	38
Figure 2.28	Grouted splice sleeve [110]	39
Figure 2.29	Grouted splice sleeve incorporated in [111]	40
Figure 2.30	Typical specimen for tests on the column-to-column grouted sleeve connection used by Tullini and Minghini [6]	42
Figure 2.31	Typical geometry and reinforcing layout [119]	43
Figure 2.32	Details of the proposed grouted splice sleeve connector by [129]	44
Figure 2.33	Failure modes observed by Alias et al. [129] including (a) internal sleeve-grout, (b) bar pullout, and (c) bar fracture failures	45
Figure 2.34	Details of the proposed grouted splice sleeve connector by Alias et al. [130]	46
Figure 2.35	Details of the HSS sleeve used by Seo et al. [131]	48
Figure 2.36	Details of the test setup for HSS specimens [131]	48
Figure 2.37	Failure modes observed by Seo et al. [131]	49
Figure 2.38	The resistance mechanism of HSS [131]	49
Figure 2.39	Proposed grouted splice connection by [132]	51
Figure 2.40	Test setup and placement of the strain gauge and LVDT [132]	51
Figure 2.41	Failure modes observed by [132]	52
Figure 2.42	The BPE model [105]	53
Figure 2.43	Proposed grouted spiral connection by [133]	53
Figure 2.44	Axial pullout test setup [134]	55
Figure 2.45	Flexural pullout test setup [134]	55



Figure 2.46	Failure modes observed by [134]	56
Figure 2.47	Proposed grouted splices (a) AS-series, (b) BS-series, (c) CS-series, and (d) DS-series [91]	57
Figure 2.48	Types of failure mode: (a) sleeve tensile failure, (b) grout-sleeve bond failure, (c) bar-grout bond failure, and (d) bar tensile failure [91]	59
Figure 2.49	Detail of grouted splice specimens by Einea [18]	60
Figure 2.50	Free body diagram of confinement stress generated by grouted splice [18]	61
Figure 2.51	Two types of bar splice sleeve tested by Henin and Morcoux [136]	62
Figure 2.52	Failure modes observed by Henin and Morcoux [136]	63
Figure 2.53	Finite element models of grouted splice sleeves developed by Henin and Morcoux [136]	64
Figure 2.54	Stress distribution of grouted splice sleeves developed by Henin and Morcoux [136]	64
Figure 2.55	Typical types of bond tests [32]	65
Figure 2.56	Effects of bearing stress compared with the proposed DTP-BT [45]	66
Figure 2.57	Experimental test setup by Einea [18]	67
Figure 3.1	Flowchart Showing Different Phases of the Research	71
Figure 3.2	Flowchart of Phase 1 of this Research	72
Figure 3.3	Flowchart of Phases 2 and 3 of this Research	73
Figure 3.4	Different types of specimens	75
Figure 3.5	Different types of proposed specimens	77
Figure 3.6	Control specimens, K-B series	80
Figure 3.7	Control specimens, K-P series	80
Figure 3.8	Design parameters of K-P series	80
Figure 3.9	Different parts of K-W grouted splices	81
Figure 3.10	Design parameters of K-W grouted splices	81
Figure 3.11	Control specimens of flexible aluminum sleeves, K-R Series	82
Figure 3.12	Control specimens of rigid aluminum sleeves, K-F series	82
Figure 3.13	R-FRP specimens	83
Figure 3.14	Design parameters of R-FRP grouted splices	83
Figure 3.15	F-FRP specimens	85

Figure 3.16	Design parameters of F-FRP grouted splices	85
Figure 3.17	Design parameters of T-FRP grouted splices	86
Figure 3.18	Tapered GFRP sleeves (T-FRP series)	87
Figure 3.19	Preparation of R-FRP and F-FRP sleeves	88
Figure 3.20	Preparation of T-FRP sleeves	89
Figure 3.21	Preparation of K-W series by placing smaller pipes and welding the bolts	90
Figure 3.22	Installation and placement of grouted splices	91
Figure 3.23	Grouting and installation of the upper reinforcement bar	91
Figure 3.24	R-C and R-G series	92
Figure 3.25	Placement of strain gauges	92
Figure 3.26	Placement of strain gauges, F-G series	93
Figure 3.27	Typical elements of grouted splice specimen	94
Figure 3.28	Woven roving E-glass fibers	97
Figure 3.29	Woven roving carbon fibers	97
Figure 3.30	Test setup, strain gauge placement	99
Figure 3.31	Data acquisition system	100
Figure 3.32	FRP composite coupons	101
Figure 4.1	LVDT placement to measure ultimate displacement of grouted splices	114
Figure 4.2	Load-displacement responses of control specimens	116
Figure 4.3	Load-displacement responses of R-FRP grouted splices	116
Figure 4.4	Load-displacement responses of F-FRP grouted splices	117
Figure 4.5	Load-displacement responses of T-FRP grouted splices	117
Figure 4.6	Strain gauge placement of the specimens	118
Figure 4.7	Stress-strain responses of R-FRP grouted splices	119
Figure 4.8	Stress-strain responses of F-FRP grouted splices	119
Figure 4.9	Stress-strain responses of T-FRP grouted splices	120
Figure 4.10	Stress-strain responses of R-FRP grouted splices	120
Figure 4.11	Stress-strain responses of F-FRP grouted splices	121
Figure 4.12	Stress-strain responses of T-FRP grouted splices	121
Figure 4.13	Stress-strain responses of R-C series	123
Figure 4.14	Stress-strain responses of F-C series	123
Figure 4.15	Stress-strain responses of R-G series	124

Figure 4.16	Grout bond slip failure	125
Figure 4.17	Mechanism of bar bond-slip failure	126
Figure 4.18	Crushing of the grout in front of the rib as bar slips (Gray: displaced rib position)	127
Figure 4.19	Bar bond-slip failure of specimen R-C <sub>6</sub> L <sub>125</sub> -1	127
Figure 4.20	Stress distribution (modified from Ferguson et al.) [25]	128
Figure 4.21	Aluminum tube bond-slip failure of specimen F-G <sub>6</sub> L <sub>125</sub> -1	129
Figure 4.22	Sleeve fracture failure	131
Figure 4.23	Bar fracture	132
Figure 4.24	Pre-yield, post-yield, and yield point of specimens failed in ductile manner	134
Figure 4.25	Pre-yield, post-yield, and yield point of specimens with brittle behavior	135
Figure 4.26	Comparison of stiffness between: (a) control specimen and (b) FRP grouted splice	136
Figure 4.27	Mechanism of Bond Resistance in Confined Concrete: (a) inclined cracks at steel lugs; (b) crushing and shear cracks of grout keys; and (c) progressive shearing-off of the grout keys	137
Figure 4.28	Mechanical interlocking mechanism of bond and componential stresses	156
Figure 4.29	Mechanism of radial crack propagation and confinement by sleeve	157
Figure 4.30	The effects of sleeve design parameters on confinement	158
Figure 4.31	Comparison between tensile strength of T-FRP, R-FRP, and F-FRP specimens	159
Figure 4.32	The sleeve design parameters in K-P, K-R, and K-F series	161
Figure 4.33	Comparison between tensile strength of R-FRP, F-FRP, and control specimens K-P, K-R, and K-F	161
Figure 4.34	Comparison between tensile strength of R-FRP, F-FRP, and control specimens	162
Figure 4.35	FRP grouted splices failed under axial and radial tension	163
Figure 4.36	Effects of sleeve diameter on tensile strength of T-FRP Specimens	165
Figure 4.37	Effects of sleeve diameter on pre-yield stiffness of T-FRP Specimens	165
Figure 4.38	Effects of inner diameter at mid-length of sleeve on bond strength of T-FRP specimens	166

Figure 4.39	Effects of bar embedded lengths on tensile strength of FRP grouted splices	167
Figure 4.40	Effects of bar embedded lengths on pre-yield stiffness of FRP grouted splices	168
Figure 4.41	Relationships between $\mu_s$ and $L_e$ of R-FRP grouted splices	170
Figure 4.42	Relationships between $\mu_s$ and $L_e$ of F-FRP grouted splices	171
Figure 4.43	Relationships between $\mu_s$ and $L_e$ of T-FRP grouted splices	171
Figure 4.44	Comparison between minimum embedded lengths proposed by graphical and ultimate bond stress methods	177
Figure 4.45	Free body diagram of stress in the grouted splices suggested by Einea [18]	177
Figure 4.46	Free body diagram of stress of the FRP grouted splice connection used in this study	178
Figure 4.47	Relationship of $\tau/\sqrt{f_g}$ versus $\sqrt{\sigma_{n,b}}$ [24]	181
Figure 4.48	Comparison of predicted values of ultimate tensile load by Equations 4.59 and 4.60 versus experimental values	185
Figure 5.1	Schematic drawing of the components of a biological neuron [150]	191
Figure 5.2	Schematic diagram of ANN models in this study	194
Figure 5.3	Mean Squared Error (MSE) versus numbers of hidden layer neurons	196
Figure 5.4	Regression value (R) versus NN 5-n-1	197
Figure 5.5	Performance of NN 5-10-1	197
Figure 5.6	Training state of NN 5-10-1	198
Figure 5.7	Regressions of training, validation and test data simulated by NN 5-10-1	199
Figure 5.8	Comparison of various predicted values of $P_u$ versus experimental data for NN5-10-1	200
Figure 5.9	Comparison of various predicted values of $P_u$ versus experimental data for Equation 6.2 to 6.4	201
Figure 5.10	Comparison of various predicted values of $P_u$ versus experimental data for all models	201
Figure 5.11	Schematic diagram of NN4-10-1 for cylindrical CFRP and GFRP specimens	209
Figure 5.12	Schematic diagram of NN5-10-1 for tapered GFRP Specimens	209
Figure 5.13	Performance of optimal neural networks	210
Figure 5.14	Training state of optimal neural networks	211

Figure 5.15	(a) Regressions of training, validation and test data simulated by NN4-10-1 for cylindrical CFRP specimens	212
Figure 5.15	(b) Regressions of training, validation and test data simulated by NN4-10-1 for cylindrical CFRP specimens	212
Figure 5.15	(c) Regressions of training, validation and test data simulated by NN5-10-1 for tapered GFRP specimens	213
Figure 5.16	The experimental and analytical responses of the grouted Splices	216
Figure 5.17	Schematic diagram of NN5-10-1 for all specimens	217
Figure 5.18	Performance of NN 5-10-1	217
Figure 5.19	Training state of NN 5-10-1	217
Figure 5. 20	Regression of training, validation, and test data simulated by NN 5-10-1	218
Figure 5.21	Comparison of predicted values of incremental tensile load by ANN versus experimental values	219
Figure 5.22	Comparison of predicted values of incremental tensile load by Equations 5.35, 5.36, and 5.37 versus experimental values	219
Figure 5.23	Comparison between experimental load-displacement behavior of specimens (a) R-C <sub>7</sub> L <sub>125</sub> -1 and (b) R-G <sub>7</sub> L <sub>125</sub> -2, with the predicted behavior by neural networks and Equations 5.5 and 5.6.	220
Figure 5.24	Comparison between experimental load-displacement behavior of specimens (a) F-C <sub>7</sub> L <sub>175</sub> -2 and (b) F-G <sub>6</sub> L <sub>175</sub> -1, with the predicted behavior by neural networks and Equations 5.7 and 5.8.	224
Figure 5.25	Comparison between experimental load-displacement behavior of specimens (a) T-G <sub>5</sub> D <sub>75</sub> L <sub>125</sub> -1 and (b) T-G <sub>4</sub> D <sub>50</sub> L <sub>175</sub> -1, with the predicted behavior by neural networks and Equations 5.9 and 5.10.	227
Figure 6.1	PLANE182 and PLANE183 solid elements [174]	236
Figure 6.2	The geometry of 4-node PLANE182 element [174]	237
Figure 6.3	The geometry of 8-node or 6-node PLANE183 element [174]	238
Figure 6.4	Typical stress-strain curve for the Sika grout 215	239
Figure 6.5	Simplified stress-strain curve for the grout used in finite element model	240
Figure 6.6	Applied graph of the GFRP and CFRP materials	241
Figure 6.7	The stress-strain relationship of the aluminum material	242

Figure 6.8	The simplified stress-strain relationship of the aluminum Material	242
Figure 6.9	Simplified stress-strain curve for steel reinforcement used in finite element model	243
Figure 6.10	Finite element models of specimens R-FRP series in ANSYS®	243
Figure 6.11	Finite element models of F-FRP series in ANSYS®	244
Figure 6.12	Finite element models of K-W series in ANSYS®	245
Figure 6.13	CONTA171 2-D Surface-to-Surface Contact [174]	249
Figure 6.14	CONTA172 2-D 3-Node Surface-to-Surface Contact [174]	250
Figure 6.15	Bond-slip curve for ripped steel bars embedded in concrete	251
Figure 6.16	(a) Free mesh versus (b) mapped mesh [174]	253
Figure 6.17	Meshing and boundary conditions of R-C series in ANSYS®	254
Figure 6.18	The load-displacement pattern used in finite element Model	255
Figure 7.1	Comparison of load-displacement curves between the FE analysis and the experiments on R-FRP series	262
Figure 7.2	Comparison between load-displacement curves obtained from the experiments and the FE analysis on the flexible corrugated aluminum-FRP specimens (F-FRP Series)	264
Figure 7.3	Comparison of load-displacement curves between the FE analysis and the experiments on the K-W series	267
Figure 7.4	Von Mises stress contours for (a) R-G <sub>6</sub> L <sub>75</sub> , (b) R-G <sub>7</sub> L <sub>75</sub> , (c) R-C <sub>6</sub> L <sub>75</sub> , and (d) R-C <sub>7</sub> L <sub>75</sub> with 75 mm embedment length	271
Figure 7.5	Von Mises stress contours for (a) F-G <sub>6</sub> L <sub>75</sub> , (b) F-G <sub>7</sub> L <sub>75</sub> , (c) F-C <sub>6</sub> L <sub>75</sub> , and (d) F-C <sub>7</sub> L <sub>75</sub> with 75 mm embedment length	271
Figure 7.6	Von Mises stress contours for (a) R-G <sub>6</sub> L <sub>125</sub> , (b) R-G <sub>7</sub> L <sub>125</sub> , (c) R-C <sub>6</sub> L <sub>125</sub> , and (d) R-C <sub>7</sub> L <sub>125</sub> with 125 mm embedment length	273
Figure 7.7	Von Mises stress contours for (a) F-G <sub>6</sub> L <sub>125</sub> , (b) F-G <sub>7</sub> L <sub>125</sub> , (c) F-C <sub>6</sub> L <sub>125</sub> , and (d) F-C <sub>7</sub> L <sub>125</sub> with 125 mm embedment length	273
Figure 7.8	Von Mises stress contours for (a) R-G <sub>6</sub> L <sub>175</sub> , (b) R-G <sub>7</sub> L <sub>175</sub> , (c) R-C <sub>6</sub> L <sub>175</sub> , and (d) R-C <sub>7</sub> L <sub>175</sub> with 175 mm embedment length	274

Figure 7.9	Von Mises stress contours for (a) F-G <sub>6</sub> L <sub>175</sub> , (b) F-G <sub>7</sub> L <sub>175</sub> , (c) F-C <sub>6</sub> L <sub>175</sub> , and (d) F-C <sub>7</sub> L <sub>125</sub> with 175 mm embedment length	275
Figure 7.10	Von Mises stress contours for (a) K-WL <sub>75</sub> , (b) K-WL <sub>125</sub> , and (c) K-WL <sub>175</sub>	276

## LIST OF ABBREVIATIONS

2D	-	Two Dimensional
3D	-	Three Dimensional
ANN	-	Artificial Neural Network
CFRP	-	Carbon Fiber Reinforced Polymer
CIDB	-	Construction Industry Development Board
DCDT	-	Direct Current Differential Transformers
DTP-BT	-	Direct Tension Pullout Bond Test
FE	-	Finite Element
FRP	-	Fiber Reinforced Polymer
GFRP	-	Glass Fiber Reinforced Polymer
IBS	-	Industrialized Building Systems
LVDT	-	Linear Variable Differential Transformers
MSE	-	Mean Squared Error
NN	-	Neural Network
R	-	Regression value
WS	-	Welded and Bolted Specimens



## LIST OF SYMBOLS

$\mu_d$	-	Ductility ratio
$\mu_s$	-	Strength ratio
$\mu_y$	-	Yield ratio
$A_b$	-	Steel bar cross sectional area
$A_{b,p}$	-	Contact surface area of the bar
$A_{sl}$	-	Contact surface area of the sleeve
$A_{sl,c}$	-	Contact surface area of cylindrical sleeve
$A_{sl,t}$	-	Contact surface area of tapered head sleeve
$A_{T,sl}$	-	Effective transverse cross sectional area of the sleeve
$c$	-	Constant
$d_i$	-	Inner diameter at mid-length of sleeve
$d_o$	-	Inner diameter at the end of sleeve
$E$	-	Modulus of elasticity
$E_g$	-	Modulus of elasticity of grout
$E_{sl}$	-	Modulus of elasticity of the sleeve
$f_{bt}$	-	Bond stress
$f'_c$	-	Concrete compressive strength
$f'_g$	-	Grout compressive strength
$f_n$	-	Lateral confining pressure
$F_n$	-	Confinement force
$F_{n,c}$	-	Confinement force generated in cylindrical sleeve
$F_{n,t}$	-	Confinement force generated in tapered head sleeve
$k_1$	-	Pre-yield stiffness
$k_2$	-	Post-yield stiffness
$l_e$	-	Embedded length
$l_{opt,cr}$	-	Minimum embedded length (ultimate method)
$l_{opt,gr}$	-	Minimum embedded length (graphical method)
$l_s$	-	Sleeve length

$m$	-	Slope of the regression line
$P$	-	Load
$P_{cr}$	-	Minimum requirement for the tensile strength
$P_{exp}$	-	Load recorded in experiment
$P_{NN}$	-	Load predicted by neural network
$P_{T,sl}$	-	Transverse tensile force
$P_u$	-	Ultimate tensile strength
$P_{u,exp}$	-	Experimental ultimate tensile strengths
$P_{u,FE}$	-	Fe analysis tensile strength
$P_{u,Pre}$	-	Ultimate tensile strengths predicted by proposed equations
$P_{u,NN}$	-	Ultimate tensile strengths predicted by neural network
$P_y$	-	Yield point
$S_l$	-	Slippage corresponding to the bond stress
$t$	-	Thickness
$t_{frp}$	-	Thickness of fiber reinforced polymer
$t_{sl}$	-	Sleeve thickness
$T$	-	Bond strength
$T_c$	-	Bond strength of cylindrical specimen
$T_s$	-	Tangential force
$T_t$	-	Bond strength of tapered specimen
$U$	-	Bond strength of concrete
$x$	-	Normalized data
$X_{max}$	-	Minimum value of variable
$X_{min}$	-	Maximum value of variable
$\Delta l$	-	Small longitudinal length
$\Delta_u$	-	Ultimate displacement
$\Delta_{u,Exp}$	-	Experimental ultimate displacement
$\Delta_{u,FE}$	-	FE Analysis ultimate displacement
$\Delta_y$	-	Displacement at yield
$\varepsilon_s$	-	Tangential strain
$\varepsilon_{T,sl}$	-	Tensile strain of sleeve
$\vartheta$	-	Poisson's ratio

$\nu_s$	-	Poisson's ratio of grout
$\rho$	-	Mass density
$\sigma_n$	-	Normal confinement stress
$\sigma_{n,b,c}$	-	Normal confinement stress of cylindrical sleeve
$\sigma_{n,b,t}$	-	Normal confinement stress of tapered sleeve
$\sigma_{sy}$	-	Yield stress
$\sigma_{T,sl}$	-	Transverse tensile stress of sleeve
$\sigma_u$	-	Ultimate tensile stress
$\sigma_y$	-	Specified yield strength
$\tau$	-	Bond stress
$\tau_{cr}$	-	Ultimate bond stress
$\tau_{max}$	-	Maximum bond strength
$\tau_{u,Exp}$	-	Experimental bond stress
$\tau_{u,NN}$	-	Bond stress predicted by neural networks
$\varphi$	-	Bar diameter

## LIST OF APPENDICES

<b>APPENDIX</b>	<b>TITLE</b>	<b>PAGE</b>
Appendix A	Fabrication of the Grouted Splice Connections	300
Appendix B	Failure Modes of the Grouted Splice Connections	322
Appendix C	Load-Displacement Responses of FRP Grouted Splice Connections	330
Appendix D	Transverse Tensile Strains of FRP Grouted Splice Connections	333
Appendix E	ANN Model of the Load-Displacement Behavior of FRP Grouted Splice Connections	341

# CHAPTER 1

## INTRODUCTION

### 1.1 Introduction

Numerous advantages of precast concrete systems made them a promising alternative choice to their conventional reinforced concrete counterparts in the construction industry. Precast concrete systems have the potential to increase the quality of building components by producing them under the controlled environment. Moreover, the precast systems can provide significant benefits for engineers, labors, and public by improving the quality, constructability, work zone safety and minimizing the environmental impacts, construction costs, and traffic disruptions. In this regard, the main objective of Construction Industry Development Board (CIDB) of Malaysia is to develop the capacity and capability of the construction industry through enhancing the quality and productivity by expanding the employment of precast concrete systems [1].

The chronology of the Industrialized Building Systems (IBS) in Malaysia goes back to 1960s. Sufficient exposure and incentives are pouring in to encourage industry players to make a paradigm move – from conventional to IBS construction. In this regard, about 22.7 acres of land in Jalan Pekeliling, Kuala Lumpur was dedicated to the first IBS project during the 1<sup>st</sup> and 2<sup>nd</sup> Malaysian Plan (1960–1965 and 1966–1970) to build quality and affordable houses in a shorter period of time. This project comprised of 7 blocks of 17 stories flat consisted of 3000 units of low-cost flat and 40 shops lot [2-4]. Due to the problems related with some of the foreign prefabricated systems in 1960s and 1970s, identifying newer, better, and innovative technologies which are suitable with Malaysian climate and social practices has been the main objective for the construction industry in Malaysia. To promote the IBS

usage in the industry, the IBS Strategic Plan was introduced in 1999 [2]. This was followed by developing IBS Roadmaps 2003-2011 and 2011-2015 to enhance the efficiency, quality, sustainability, competency and research and development programs. To increase the contribution of the IBS industry, the Malaysian government mandated that all public-sector projects must attain no less than 70% IBS-content under the Treasury Circular SPP 07/2008 [1].

In recent years, IBS precast components are used in construction projects to offer solutions to overcome the increasing demands for schools, hospitals, colleges, universities and private buildings. It was only possible through expanding knowledge through intensive research on local IBS technologies.

The connections are the most important components of precast concrete systems, as the overall integrity of the precast structure is largely governed by its connections. Connections alone can dictate the type of precast frame, the limitations of that frame, and the erection progress which emphasizes the importance of connections in precast concrete systems [5,6]. Hence, addressing the effectiveness of precast connections in transferring the forces between individual building components (is a research area that) needs further investigations. In this regard, current research is carried out to develop and study grouted splice connections to join precast concrete components.

There are different ways to have a satisfactory connection, such as welding, bolting, or grouting. The used method should be simple and applicable on site. Grouted splice connections can be completed much faster with significant reduction in the required embedded length of the reinforcement bars compared to conventional methods such as cast-in-place concrete [4]. This fact makes the splice connections a good choice for heavily reinforced structures.

There are two different types of connections: conventional method or lapping reinforcement bar, and mechanical connections. Grout filled splices connection is a form of mechanical connection which have been used to connect precast members

and they have been used to overcome the issues related to the long embedded length of lapping systems. During the fabrication, sleeves are pre-embedded in one end of the precast member and projecting steel bars are inserted into the sleeves to fit two sides of the members. Then, the space between the bars and sleeves is filled with non-shrink grout (see Figure 1.1). By having a good installation of the connection, the sleeves can withstand applied forces and they can develop the full strength of the bars to have a monolithic behavior as cast in situ concrete.

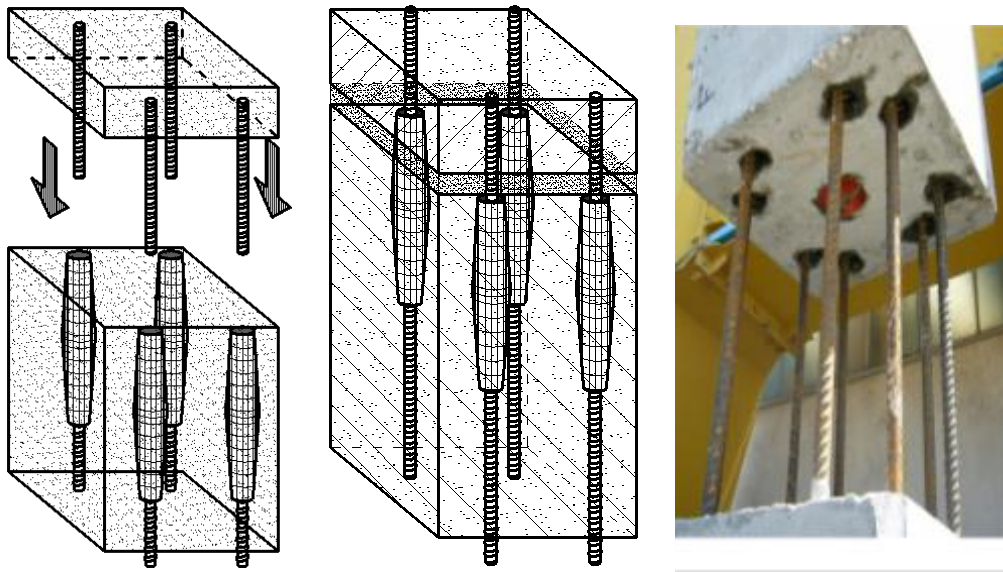


Figure 1.1 Installation of grouted splice connections [6]

Several types mechanical connections are available on the market such as Lenton Interlok® [7, 8], NMB Splice-Sleeve® [9], Quick-Wedge©, BarSplice Products Inc, etc. The main problem related to such proprietary products is that little information has been published about the mechanism of the connection system. Moreover, they could only be purchased from certain companies which belong to foreign countries, therefore developing a new type of sleeve connection which could be cost effective and simple to produce is necessary for countries like Malaysia.

The effectiveness of the splice connection largely depends on the generated bond between reinforcement bar and the surrounding grout. Hence, a satisfactory splice connection should be able to provide structural continuity by providing

adequate bond strength with short development length. In this regard, six types of splice connections were introduced in this research to study the factors that might affect their behaviors and feasibility under incremental tensile load.

## **1.2 Problem Statement**

Components in precast concrete systems are prefabricated, so lapping length may not be appropriate for precast concrete systems as the lapping method requires significant lapping length. Although the general structural behavior of precast components is similar to members that are monolithically cast in place, the major difference is the nature of connections. Hence, details of precast concrete connections are especially important to ensure equivalent behavior of a conventionally designed, cast-in-place, monolithic concrete structure [10]. While the continuity in cast-in-place systems is achieved by providing lapped reinforcement bars to have a monolithic system, it can be achieved by utilizing grouted splice connections with shorter anchorage lengths in precast systems.

However, limited information is provided by design codes as practical solutions for designing a splice connection which might be due to the proprietary and confidential nature of these products. On the other hand, available studies about the performance of the spliced connections are restricted to the small scale experimental studies with limited design parameters which might not be suitable to predict the acceptability of the connections [11-13].

Furthermore, the majority of the published articles are mainly focused on grouted splices produced from steel pipes. Steel pipes cannot generate required interlocking mechanism between their inner surface and the grout. Hence, several methods have been used by previous researches to provide adequate interlocking mechanism. Among the proposed methods, welding gained more attention due to its advantage over other methods like threading. This might be due to this fact that compared to best-quality thread, providing interlocking mechanism by welding is



cost effective and it permits the use of thinner pipes as it does not cause mechanical weakening.

The issues related to the research are:

1. The embedded lengths used in precast grouted splice connections are much shorter than the embedded lengths offered by design standards. Hence, ensuring the ability of the grouted splice to develop the full strength capacity and maintaining the structural continuity of the spliced bars is a critical issue in practice. In this regard, further research is required to study the acceptability of the short embedded lengths and subsequently identifying the minimum bar embedded lengths of the grouted splices able of developing full tensile strengths of the spliced bars.
2. During the design process, if the ultimate strength of the grouted splice connection is not determined precisely, it may lead to catastrophic failures in the structure. In order to obtain reliable predictions of the ultimate strength of the grouted splices with different design parameters, analytical research are conducted and equations are derived by analyzing the experimental results of the current study.
3. In practice, predicting the behavior of the grouted splice is the key issue to assure designers and contractors in using grouted splices. To do this, an extensive experimental and analytical research is carried out to justify the load responses of the grouted splices with different design parameters under incremental tensile load.
4. The majority of the published studies are limited to conventional steel products and they did not cover the practicality of the alternative materials and design parameters. Hence, further investigation is required to understand the effects of different combination of confining materials on the performance and behavior of the spliced connections.

### **1.3 Objectives**

The specific objectives of the research are:

1. To study experimentally the behavior, performance, and satisfactory design parameters of the proposed grouted splice connections using FRP sheets as the confinement and subjected to incremental tensile load.
2. To develop empirical relationship of the behavior of the proposed grouted splices based on the experimental results.
3. To predict the behavior and performance of the proposed FRP grouted splice connections using Artificial Neural Network (ANN).
4. To investigate the behavior of the FRP grouted splice connection such as load-displacement, types of failure, and ultimate tensile strength using Finite Element Method (FEM).
5. To compare the results of the proposed empirical relationship, neural network model, and finite element method with the experimental results of the proposed FRP grouted splice connections.

### **1.4 Scopes of Research**

The scope of the research program is limited to the following:

1. Steel reinforcement bars with diameter of 16 mm were used for all grouted splices.
2. The sleeve diameter of the proposed grouted splices ranging from 37 mm to 75 mm.
3. The embedded lengths of 75 mm, 125 mm, and 175 mm were considered for the proposed grouted splices.
4. One type of grout was used to prepare the proposed grouted splices.

5. Mild steel pipes, two types of aluminum tubes (rigid and flexible corrugated tubes), glass and carbon fiber reinforced polymers were used to prepare the proposed grouted splices.
6. Grouted splices were subjected to incremental tensile load and other load cases were not considered.
7. Artificial neural network and finite element methods were used to predict the behavior and performance of FRP grouted splice connections only.

## **1.5 Thesis Outline**

The general aim of this thesis was to study the behavior of the grouted splice connections under incremental tensile load until failure. This thesis comprises of eight chapters covering three phases of this study.

A brief introduction of the grouted splice connections, relative problem statement, the objectives and scopes of this study are presented in Chapter 1.

Chapter 2 presents the review of the available literature and the present state of knowledge regarding grouted connections and proposed methods for studying and analyzing the behavior of these type of connections.

Chapter 3 describes the experimental program, including the details of test specimens, different variables considered in the proposed connections, material specifications, instrumentations, test setup and procedures.

Chapter 4 covers Phase 1 of this study and presents the results and discusses the effects of various designs on the responses of the grouted splice connections when subjected to incremental tensile load. Moreover, an empirical relationship was developed in this phase of research to verify and predict the ultimate strength as well as the load-displacement responses of the grouted splices under incremental tensile load.

## REFERENCES

1. Kamar, K.A.M., et al. *Industrialised Building Systems (IBS): A review of experience in UK and Malaysia construction industry*. in *2nd Construction Industry Research Achievement International Conference (CIRAIC)*, Kuala Lumpur, Malaysia. 2009.
2. Thanoon, W., et al. *The Experiences of Malaysia and other countries in industrialised building system*. in *Proceeding of International Conference on Industrialised Building Systems*, Sep. 2003.
3. Kamar, K., M. Alshawi, and Z. Hamid. *Barriers to industrialized building system (IBS): The case of Malaysia*. in *BuHu 9th International Postgraduate Research Conference*. 2009.
4. Rahman, A.B.A. and W. Omar. *Issues and challenges in the implementation of industrialised building systems in Malaysia*. in *Proceedings of the 6th Asia-Pacific structural Engineering and Construction Conference (Apscc 2006)*, Kuala Lumpur. Malaysia. 2006. Citeseer.
5. Elliott, K.S., *Precast concrete structures*. 2016: Crc Press.
6. Tullini N, Minghini F. *Grouted sleeve connections used in precast reinforced concrete construction—Experimental investigation of a column-to-column joint*. *Engineering Structures*. 2016 Nov 15;127:784-803.
7. Albrigo, J., E.D. Ricker, and L.J. Colarusso, *Method of forming concrete structures with a grout splice sleeve which has a threaded connection to a reinforcing bar*. 1994, Google Patents.
8. Albrigo, J., E.D. Ricker, and L.J. Colarusso, *Reinforcing bar splice and system for forming precast concrete members and structures*. 1995, Google Patents.
9. Yee, A.A., *Splice sleeve for reinforcing bars*. 1970, Google Patents.
10. Austin, R., et al., *Emulating Cast-in-Place Detailing in Precast Concrete Structures*. Farmington Hills, MI, 2001. 16.
11. Jansson PO. *Evaluation of grout-filled mechanical splices for precast concrete construction*. Michigan Department of Transportation MDOT; 2008.
12. Coogler, K.L., K.A. Harries, and M. Gallick, *Experimental study of offset mechanical lap splice behavior*. *ACI Structural Journal*, 2008. **105**(4): p. 478.
13. TokyoSteelCorp, *Tokyo Steel Corp*. BCJ-C1659, 1994.
14. Council, B.S.S., *National Earthquake Hazard Reduction Program (NEHRP) recommended provisions for seismic regulations for 348 new buildings and other structures—part 2: commentary (FEMA 450-2)*. Federal Emergency Management Agency, Washington, DC, 2003.
15. Goetsch, D.L., *Structural, Civil and Pipe Drafting*. 2013: Cengage Learning.
16. Negro, P. and G. Toniolo, *Design Guidelines for Connections of Precast Structures under Seismic Actions Third Main Title Line Third Line*. 2012.

17. Lancelot, H.B., *Mechanical splices of reinforcing bars*. CONCRETE CONSTRUCTION, 1985. **30**(1): p. 23-&.
18. Einea, A., T. Yamane, and M.K. Tadros, *Grout-filled pipe splices for precast concrete construction*. PCI journal, 1995. **40**(1): p. 82-93.
19. McDermott, J., *Mechanical Connections of Reinforcing Bars*. ACI Structural Journal, 1991. **88**(2): p. 222-237.
20. NMB Splice Sleeve System User's Manual. 2007.
21. 116, A.C., *Cement and concrete terminology*. 1985: American Concrete Institute.
22. Loh, H.Y., *Development of Grouted Splice Sleeve and Its Performance Under Axial Tension*. 2008: Universiti Teknologi Malaysia.
23. Thompson, M., et al., *Anchorage behavior of headed reinforcement: Literature review*. 2002.
24. Untrauer, R.E. and R.L. Henry. *Influence of normal pressure on bond strength*. in Journal Proceedings. 1965.
25. Ferguson PM, Breen JE, Jirsa JO. *Reinforced concrete fundamentals*. John Wiley & Sons, Inc.; 1988.
26. Goto, Y. *Cracks formed in concrete around deformed tension bars*. in Journal Proceedings. 1971.
27. Mains RM. *Measurement of the distribution of tensile and bond stresses along reinforcing bars*. ACI J Proc 1951; **48**(11):225–52.
28. Jiang, D., S. Shah, and A. Andonian. *Study of the transfer of tensile forces by bond*. in Journal Proceedings. 1984.
29. BSI, B.S., 8110-1: 1997. *Structural use of concrete–Part 1: Code of practice for design and construction*.
30. Brenes, F.J., S.L. Wood, and M.E. Kreger, *Anchorage requirements for grouted vertical-duct connectors in precast bent cap systems*. 2006.
31. Feldman, L.R. and F.M. Bartlett, *Bond strength variability in pullout specimens with plain reinforcement*. ACI Structural Journal, 2005. **102**(6): p. 860.
32. Abrishami, H.H. and D. Mitchell, *Analysis of bond stress distributions in pullout specimens*. Journal of Structural Engineering, 1996. **122**(3): p. 255-261.
33. Robins, P. and I. Standish, *The influence of lateral pressure upon anchorage bond*. Magazine of Concrete Research, 1984. **36**(129): p. 195-202.
34. Lutz, L.A., *The Mechanics Of Bond And Slip Of Deformed Reinforcing Bars In Concrete*. 1968.
35. Cox, J.V. and L.R. Herrmann, *Development of a plasticity bond model for steel reinforcement*. Mechanics of Cohesive-frictional Materials: An International Journal on Experiments, Modelling and Computation of Materials and Structures, 1998. **3**(2): p. 155-180.
36. Moosavi, M., A. Jafari, and A. Khosravi, *Bond of cement grouted reinforcing bars under constant radial pressure*. Cement and Concrete Composites, 2005. **27**(1): p. 103-109.

37. ACI Committee, A., *Bond and Development of Straight Reinforcing Bars in Tension (ACI 408R-03)*. American Concrete Institute, Detroit, Michigan, US, 2003: p. 49.
38. Mander, J.B., M.J. Priestley, and R. Park, *Theoretical stress-strain model for confined concrete*. Journal of structural engineering, 1988. **114**(8): p. 1804-1826.
39. Hungspreug, S., *Local Bond Between A Steel Bar And Concrete Under High Intensity Cyclic Load*. 1981.
40. Tassios, T. and I. Vassilopoulou, *Shear transfer capacity along a RC crack, under cyclic sliding*. Befestigungstechnik Bewehrungstechnik, (Rolf Eligehausenzum 60. Geburtstag), (eds. W. Fuchs, HW Reinhardt), Ibidem-Verlag, Stuttgart, 2002: p. 405-414.
41. Pfister, J.F. and A.H. Mattock, *High strength bars as concrete reinforcement, part 5: lapped splices in concentrically loaded columns*. Vol. 63. 1963: Portland Cement Association, Research and Development Laboratories.
42. Pfister, J.F. *Influence of ties on the behavior of reinforced concrete columns*. in Journal Proceedings. 1964.
43. Alavi-Fard, M. and H. Marzouk, *Bond of high-strength concrete under monotonic pull-out loading*. Magazine of Concrete Research, 2004. **56**(9): p. 545.
44. Soroushian, P., et al., *Bond of deformed bars to concrete: effects of confinement and strength of concrete*. Materials Journal, 1991. **88**(3): p. 227-232.
45. Tastani, S. and S. Pantazopoulou, *Experimental evaluation of the direct tension-pullout bond test*. Bond in Concrete—from research to standards, Budapest; 2002.
46. Loo, G.K., *Parametric study of grout-filled splice sleeve integrated with flexible aluminium tube for precast concrete connection*. 2009, Universiti Teknologi Malaysia.
47. Lim, C.T., *The Effects of Pitch Distance of Steel Spiral Reinforcement to the Performance of Grouted Sleeve Connector Under Direct Tensile Load*. 2010, Universiti Teknologi Malaysia.
48. Tibbetts, A.J., M.G. Oliva, and L.C. Bank, *Durable fiber reinforced polymer bar splice connections for precast concrete structures*. Composites & ploycon, 2009: p. 15-17.
49. Soroushian, P. and K.-B. Choi, *Local bond of deformed bars with different diameters in confined concrete*. Structural Journal, 1989. **86**(2): p. 217-222.
50. Chaallal, O. and B. Benmokrane, *Pullout and bond of glass-fibre rods embedded in concrete and cement grout*. Materials and structures, 1993. **26**(3): p. 167-175.
51. Chaallal, O. and B. Benmokrane, *Physical and mechanical performance of an innovative glass-fiber-reinforced plastic rod for concrete and grouted anchorages*. Canadian Journal of Civil Engineering, 1993. **20**(2): p. 254-268.

52. Cosenza, E., G. Manfredi, and R. Realfonzo, *Behavior and modeling of bond of FRP rebars to concrete*. Journal of composites for construction, 1997. **1**(2): p. 40-51.
53. GangaRao, H., et al., *FRP composites applications for non-ductile structural systems: short-and long-term behavior*. Report Submitted to (CEERD-CT-T)-US Army Corps of Engineers. Double layer of U-wrap at end of NSM rebar, 2001.
54. Farndon, S., *Effect of Normal Pressure on Bond in Lightweight Concrete*. Department of Civil Eng., Loughborough University, 1982.
55. Tepfers R. *A theory of bond applied to overlapped tensile reinforcement splices for deformed bars*. Chalmers University of Technology; 1973.
56. Standish, I.G., *The effect of lateral pressure on anchorage bond in lightweight aggregate concrete*. 1982, © Ian Guy Standish.
57. St John NA, Brown JR. *Flexural and interlaminar shear properties of glass-reinforced phenolic composites*. Composites Part A: Applied Science and Manufacturing. 1998 Aug 1; **29**(8):939-46.
58. Callus PJ, Mouritz AP, Bannister MK, Leong KH. *Tensile properties and failure mechanisms of 3D woven GFRP composites*. Composites Part A: applied science and manufacturing. 1999 Nov 1; **30**(11):1277-87.
59. Degallaix G, Hassaini D, Vittecoq E. *Cyclic shearing behaviour of a unidirectional glass/epoxy composite*. International journal of fatigue. 2002 Feb 1; **24**(2-4):319-26.
60. Vlot A, Gunnink JW, editors. *Fibre metal laminates: an introduction*. Springer Science & Business Media; 2011 Jun 28.
61. Tarnopol'skii YM, Arnautov AK, Kulakov VL. *Methods of determination of shear properties of textile composites*. Composites Part A: Applied Science and Manufacturing. 1999 Jul 1; **30**(7):879-85.
62. Rikards R. *Interlaminar fracture behaviour of laminated composites*. Computers & Structures. 2000 Jun 1; **76**(1-3):11-8.
63. Kawai M, Hachinohe A, Takumida K, Kawase Y. *Off-axis fatigue behaviour and its damage mechanics modelling for unidirectional fibre-metal hybrid composite: GLARE 2*. Composites Part A: Applied Science and Manufacturing. 2001 Jan 1; **32**(1):13-23.
64. Soprano A, Apicella A, D'Antonio L, Schettino F. *Application of durability analysis to glare aeronautical components*. International journal of fatigue. 1996 May 1; **18**(4):265-72.
65. Uenal O, Barnard DJ, Anderson IE. *A shear test method to measure shear strength of metallic materials and solder joints using small specimens*. Scripta Materialia. 1999 Jan 8; **40**(3).
66. Chiang MY, He J. *An analytical assessment of using the losipescu shear test for hybrid composites*. Composites Part B: Engineering. 2002 Sep 1; **33**(6):461-70.

67. Kawai M, Morishita M, Tomura S, Takumida K. *Inelastic behavior and strength of fiber-metal hybrid composite: Glare*. International Journal of Mechanical Sciences. 1998 Feb 1; **40**(2-3):183-98.
68. Naboulsi S, Mall S. *Thermal effects on adhesively bonded composite repair of cracked aluminum panels*. Theoretical and applied fracture mechanics. 1997 Jan 1; **26**(1):1-2.
69. Asnafi N, Langstedt G, Andersson CH, Östergren N, Håkansson T. *A new lightweight metal-composite-metal panel for applications in the automotive and other industries*. Thin-walled structures. 2000 Apr 1; **36**(4):289-310.
70. Asundi A, Choi AY. *Fiber metal laminates: an advanced material for future aircraft*. Journal of Materials processing technology. 1997 Jan 1; **63**(1-3):384-94.
71. Wittenberg TC, Van Baten TJ, De Boer A. *Design of fiber metal laminate shear panels for ultra-high capacity aircraft*. Aircraft Design. 2001 Jun 1; **4**(2-3):99-113.
72. Vlot A, Fredell RS. *Impact damage resistance and damage tolerance of fibre metal laminates*. Proceedings of the ICCM/9 Madrid. 1993; **6**:51-8.
73. Botelho EC, Silva RA, Pardini LC, Rezende MC. *A review on the development and properties of continuous fiber/epoxy/aluminum hybrid composites for aircraft structures*. Materials Research. 2006 Sep; **9**(3):247-56.
74. Zweben C. *Mechanical behaviour and properties of composite materials*. Delaware Composite Design Encyclopedia. 1989; 1.
75. Proust G. *Adhesion of protective coating appliques on contaminated aluminum surfaces*. 2002.
76. Wu G, Yang JM. *The mechanical behavior of GLARE laminates for aircraft structures*. Jom. 2005 Jan 1; **57**(1):72-9.
77. Alderliesten RC, Homan JJ. *Fatigue and damage tolerance issues of Glare in aircraft structures*. International Journal of Fatigue. 2006 Oct 1; **28**(10):1116-23.
78. Vlot A. *Impact loading on fibre metal laminates*. International Journal of Impact Engineering. 1996 Apr 1; **18**(3):291-307.
79. Krishnakumar S. *Fiber metal laminates-the synthesis of metals and composites*. Material And Manufacturing Process. 1994 Mar 1; **9**(2):295-354.
80. Abdullah MR, Prawoto Y, Cantwell WJ. *Interfacial fracture of the fibre-metal laminates based on fibre reinforced thermoplastics*. Materials & Design. 2015 Feb 5; **66**:446-52.
81. Carrillo JG. *A study of the mechanical properties and scaling effects in a thermoplastic fibre-metal laminate*. Doctoral dissertation, 2007. University of Liverpool.
82. Cortes P. *The fracture properties of a fiber metal laminate based on a self-reinforced thermoplastic composite material*. Polymer composites. 2014 Mar; **35**(3):427-34.



83. Kiratisaevee H, Cantwell WJ. *The fracture behavior of aluminum foam sandwich structures based on fiber reinforced thermoplastics*. Journal of Sandwich Structures & Materials. 2003 Jan; **5**(1):53-75.
84. Carrillo JG, Cantwell WJ. *Mechanical properties of a novel fiber-metal laminate based on a polypropylene composite*. Mechanics of Materials. 2009 Jul 1; **41**(7):828-38.
85. Li H, Hu Y, Xu Y, Wang W, Zheng X, Liu H, Tao J. *Reinforcement effects of aluminum-lithium alloy on the mechanical properties of novel fiber metal laminate*. Composites Part B: Engineering. 2015 Dec 1; **82**:72-7.
86. Wu G, Yang JM. *The mechanical behavior of GLARE laminates for aircraft structures*. Jom. 2005 Jan 1; **57**(1):72-9.
87. Lawcock G, Ye L, Mai YW, Sun CT. *The effect of adhesive bonding between aluminum and composite prepreg on the mechanical properties of carbon-fiber-reinforced metal laminates*. Composites Science and Technology. 1997 Jan 1; **57**(1):35-45.
88. Fam A, Witt S, Rizkalla S. *Repair of damaged aluminum truss joints of highway overhead sign structures using FRP*. Construction and Building Materials. 2006 Dec 1; **20**(10):948-56.
89. Wermiel SE. California Concrete, 1876-1906: Jackson, Percy, and the Beginnings of Reinforced Concrete Construction in the United States. In Proceedings of the Third International Congress on Construction History 2009 May (pp. 1509-1516).
90. Hurst BL. *Concrete And The Structural Use Of Cements In England Before 1890*. Proceedings of the Institution of Civil Engineers-Structures and Buildings. 1996 Aug; **116**(3):283-94.
91. Ling JH, Rahman AB, Ibrahim IS. *Feasibility study of grouted splice connector under tensile load*. Construction and Building Materials. 2014 Jan 15; **50**:530-9.
92. Lutz LA. *The mechanics of bond and slip of deformed reinforcing bars in concrete*. ACI J Proc 1966.
93. Hamad BS. *Comparative bond strength of coated and uncoated bars with different rib geometries*. ACI Mater J 1995; **92**(6):579-90.
94. Darwin D, Graham EK. *Effect of deformation height and spacing on bond strength of reinforcing bars*. ACI J 1993; **90**(6):646-57.
  
95. Abrams DA. *Tests of bond between concrete and steel*. Urbana: University of Illinois; 1913. p. 71.
96. Clark AP. *Bond of concrete reinforcing bars*. Detroit, Michigan; 1949.
97. Goto Y. *Cracks formed in concrete around deformed tension bars*. ACI J Proc 1971; **68**(4):244-51.
98. Gambarova PG, Rosati GP, Schumm CE. *Bond and splitting: a vexing question*. Int Concr Res Inform Portal 1998; SP-180:23-44.

99. Rosati GP, Schumm CE. *Modeling of local bar-to-concrete bond in RC beams*. In: International conference “bond in concrete: from research to practice”, Riga, Latvia; 1992.
100. Chamberlin SJ. *Spacing of spliced bars in tension pull-out specimens*. Proc J Am Concr Inst 1952; **49**(4):261–74.
101. Chinn J, Ferguson PM, Thompson JN. *Lapped splices in reinforced concrete beams*. Proc J Am Concr Inst 1955; **52**(2):201–12.
102. Orangun CO, Jirsa JO, Breen JE. A reevaluation of test data on development length and splices. ACI J 1977; **74**(3):114–22.
103. Lormanometee S. *Bond strength of deformed reinforcing bar under lateral pressure*. University of Texas at Austin; 1974.
104. Untrauer RE, Henry RL. *Influence of normal pressure on bond strength*. ACI J 1965; **65**(5):577–85.
105. Eligehausen, R., Popov, E.P., Bertero, V.V.: *Local bond stress-slip relationships of deformed bars under generalized excitations, Report No. 83R23*, EERC, University of California, Berkeley, 1983.
106. Ling JH. *Behavior of grouted splice connections in precast concrete wall subjected to tensile, shear and flexural loads*. 2011, Universiti Teknologi Malaysia.
107. Lim CT. *The effect of pitch distance of steel spiral reinforcement to the performance of grouted sleeve connector under direct tensile load*. 2010, Universiti Teknologi Malaysia.
108. Lee GS. *Parametric studies of sleeve connector using steel pipe with spiral steel for precast concrete connection*. 2009, Universiti Teknologi Malaysia.
109. Parks JE, Papulak T, Pantelides CP. *Acoustic emission monitoring of grouted splice sleeve connectors and reinforced precast concrete bridge assemblies*, Construction and Building Materials, **122**(2016) 537-47.
110. Redd SC. *Strength, durability, and application of grouted couplers for integral abutments in accelerated bridge construction projects: IOWA state university*, 2016.
111. Ameli MJ, Parks JE, Brown DN, Pantelides CP. *Seismic evaluation of grouted splice sleeve connections for reinforced precast concrete column-to-cap beam joints in accelerated bridge construction*, PCI Journal, **60**(2015) 80-103.
112. Zhu Z, Guo Z. *Experiments on hybrid precast concrete shear walls emulating monolithic construction with different amounts of posttensioned strands and different debond lengths of grouted reinforcements*, Advances in Materials Science and Engineering, 2016(2016) 13p.
113. Qiong Y, Xin G, Yongqing F, Zhiyuan X, Xilin L. *Grouted sleeve lapping connector and component performance tests*, Revista Tecnicade la Facultad de Ingenieria Universidad del Zulia, No. 6, **39**(2016) 136-45.
114. Qiong Y, Kun X, Zhiyuan X, Yongqing F, Xilin L. *Seismic Behavior of Precast Shear Walls with Vertical Reinforcements Overlap Grouted in*

- Constraint Sleeve*, Revista Tecnica de la Facultad de Ingenieria Universidad del Zulia, **39**(2016)207-17.
115. Yajun L, Naiyan G. *Tests on seismic behavior of pre-cast shear walls with vertical reinforcements spliced by two different grout ways*, The Open Civil Engineering Journal, **9**(2015)382-87.
  116. Sayadi AA, Rahman ABA, Jumaat MZB, Johnson Alengaram U, Ahmad S. *The relationship between interlocking mechanism and bond strength in elastic and inelastic segment of splice sleeve*, Construction and Building Materials, **55**(2014) 227-37.
  117. Sayadi AA, Rahman ABA, Jumaat MZB, Alengaram UJ, Ahmad S. *The relationship between interlocking mechanism and bond strength in elastic and inelastic segment of splice sleeve*, Construction and Building Materials, **55**(2014) 227-37.
  118. Haber ZB, Saiidi MS, Sanders DH. *Seismic Performance of Precast Columns with Mechanically Spliced Column-Footing Connections*, ACI Structural Journal, **111**(2014) 1-12.
  119. Belleri A, Riva P. *Seismic performance and retrofit of precast concrete grouted sleeve connections*, PCI Journal, **57**(2012) 97-109.
  120. ACI-318. *Building code requirements for structural concrete and commentary*. American Concrete Institute; 2002.
  121. AC-133. *Acceptance criteria for mechanical connector systems for steel reinforcing bars*. ICC Evaluation Service, Inc.; 2008.
  122. Coogler KL. *Investigation of the behavior of offset mechanical splices*. University of Pittsburgh; 2006.
  123. Quayyum, S., *Bond behavior of fibre reinforced polymer (FRP) rebars in concrete*. 2010, University of British Columbia.
  124. Ling, J.H., et al., *Performance of CS-sleeve under direct tensile load: Part I– Failure modes*. Malaysian Journal of Civil Engineering, 2008. **20**(1): p. 89-106.
  125. Xu, F., et al., *Experimental study on the bond behavior of reinforcing bars embedded in concrete subjected to lateral pressure*. Journal of Materials in Civil Engineering, 2011. **24**(1): p. 125-133.
  126. Ichinose, T., et al., *Size effect on bond strength of deformed bars*. Construction and building materials, 2004. **18**(7): p. 549-558.
  127. Ling JH, A.R.A., Abd. Hamid Z, , *Failure modes of aluminium sleeve under direct tensile load*, in 3rd International conference on postgraduate education (ICPE-3). 2008: Malaysia, Penang.
  128. Ling, J.H., et al., *Behavior of grouted pipe splice under incremental tensile load*. Construction and Building Materials, 2012. **33**: p. 90-98.
  129. Alias, Aizat & Sapawi, F & Kusbiantoro, Andri & Zubir, Mohammad & abdrahman, ahmad baharuddin. (2014). *Performance of Grouted Splice Sleeve Connector under Tensile Load*. Journal Of Mechanical Engineering And Sciences. 7. 1094-1102. 10.15282/jmes.7.2014.8.0106.

130. Alias A, Zubir MA, Shahid KA, RAhman AB. *Structural performance of grouted sleeve connectors with and without transverse reinforcement for precast concrete structure*. Procedia Engineering. 2013 Jan 1; **53**:116-23.
131. Seo SY, Nam BR, Kim SK. *Tensile strength of the grout-filled head-splice-sleeve*. Construction and building materials. 2016 Oct 15; **124**:155-66.
132. Hosseini SJ, Rahman A, Baharuddin A. *Analysis of spiral reinforcement in grouted pipe splice connectors*. Građevinar. 2013 Jul 1; **65**(06.):537-46.
133. Hosseini SJ, Rahman AB. *Effects of spiral confinement to the bond behavior of deformed reinforcement bars subjected to axial tension*. Engineering Structures. 2016 Apr 1; **112**:1-3.
134. Hosseini SJ, Rahman AB, Osman MH, Saim A, Adnan A. *Bond behavior of spirally confined splice of deformed bars in grout*. Construction and Building Materials. 2015 Apr 1; **80**:180-94.
135. Rilem/CEB/FIP. *Bond test for reinforcing steel: 1. Beam test*. Mater Struct. 1970; **3**(15) p. 169–74.
136. Henin E, Morcoux G. *Non-proprietary bar splice sleeve for precast concrete construction*. Engineering Structures. 2015 Jan 15; **83**:154-62.
137. Zhang, B. and B. Benmokrane, *Pullout bond properties of fiber-reinforced polymer tendons to grout*. Journal of materials in civil engineering, 2002. **14**(5): p. 399-408.
138. Tastani, S. and S. Pantazopoulou, *Behavior of corroded bar anchorages*. ACI Structural Journal, 2007. **104**(6): p. 756.
139. ASTM A1034 / A1034M-05, *Standard Test Methods for Testing Mechanical Splices for Steel Reinforcing Bars*. 2005, ASTM International: West Conshohocken, PA.
140. ASTM International. *Standard Test Methods and Definitions for Mechanical Testing of Steel Products*. ASTM A370 - 08b. 2008
141. Soudki, K. A. *Behaviour of Horizontal Connections for Precast Concrete Load-bearing Shear Wall Panels Subjected to reversed Cyclic Deformations*. PhD. University of Manitoba; 1994
142. BS8110 BS. *Structural use of concrete, part 1—code of practice for design and construction*. British Standards Institution, UK. 1997.
143. Soudki, S. H. R., Bill LeBlanc. *Horizontal Connections for Precast Concrete Shear Wall Subjected to Cyclic Deformations Part 1: Mild Steel Connections*. PCI Journal 1995. **41**(1): 78-96.
144. Englekirk, R. E. *Seismic Design of Reinforced and Precast Concrete Buildings*. John Wiley & Sons, Inc. 2003.
145. Chiou, Y. J., Liou, Y. W., Huang, C. C., et al. *Seismic Behavior of Precast Reinforced Concrete Walls*. 4th International Conference on Earthquake Engineering (4ICEE). Taipei, Taiwan: 2006.
146. Harajli MH, Hamad BS, Rteil AA. *Effect of confinement on bond strength between steel bars and concrete*. (vol 101, pg 595, 2004). ACI Structural Journal. 2005 May 1; **102**(3):496-496.

147. Maekawa K, Okamura H, Pimanmas A. *Non-linear mechanics of reinforced concrete*. CRC Press; 2003 Sep 2.
148. ACI Committee. *Standard tolerances for concrete construction and materials (ACI 117-90) and commentary (ACI 117R-90)*. American Concrete Institute.
149. El-Hacha R, El-Agroudy H, Rizkalla SH. *Bond characteristics of high-strength steel reinforcement*. ACI Structural Journal. 2006 Nov 1; **103**(6):771.
150. Hajela P, Berke L. *Neural networks in structural analysis and design: an overview*. Computing Systems in Engineering. 1992 Jan 1; **3**(1-4):525-38.
151. Obaidat MS. *Editorial Artificial Neural Networks To Systems, Man, And Cybernetics: Characteristics, Structures, and Applications*. IEEE Transactions on Systems, Man, and Cybernetics, Part B (Cybernetics). 1998 Aug; **28**(4):489-95.
152. Widrow B, Lehr MA. *30 years of adaptive neural networks: perceptron, madaline, and backpropagation*. Proceedings of the IEEE. 1990 Sep; **78**(9):1415-42.
153. Iranmanesh S, Mahdavi MA. *A differential adaptive learning rate method for back-propagation neural networks*. World Academy of Science, Engineering and Technology. 2009 Mar 23; **50**(1):285-8.
154. Mashrei MA, Seracino R, Rahman MS. *Application of artificial neural networks to predict the bond strength of FRP-to-concrete joints*. Construction and Building Materials. 2013 Mar 1; **40**:812-21.
155. Cevik A, Guzelbey IH. *Neural network modeling of strength enhancement for CFRP confined concrete cylinders*. Building and Environment. 2008 May 1; **43**(5):751-63.
156. Perera R, Barchín M, Arteaga A, De Diego A. *Prediction of the ultimate strength of reinforced concrete beams FRP-strengthened in shear using neural networks*. Composites Part B: Engineering. 2010 Jun 1; **41**(4):287-98.
157. Jalal M, Ramezani-pour AA. *Strength enhancement modeling of concrete cylinders confined with CFRP composites using artificial neural networks*. Composites Part B: Engineering. 2012 Dec 1; **43**(8):2990-3000.
158. Dai J, Ueda T, Sato Y. *Development of the nonlinear bond stress–slip model of fiber reinforced plastics sheet–concrete interfaces with a simple method*. Journal of composites for construction. 2005 Feb; **9**(1):52-62.
159. Tang CW, Chen HJ, Yen T. *Modeling confinement efficiency of reinforced concrete columns with rectilinear transverse steel using artificial neural networks*. Journal of Structural Engineering. 2003 Jun; **129**(6):775-83.
160. Khademi F, Behfarnia K. *Evaluation of concrete compressive strength using artificial neural network and multiple linear regression models*. Iran University of Science & Technology. 2016 Sep 15; **6**(3):423-32.
161. Sakla SS, Ashour AF. *Prediction of tensile capacity of single adhesive anchors using neural networks*. Computers & structures. 2005 Aug 1; **83**(21-22):1792-803.

162. Dahou Z, Sbartai ZM, Castel A, Ghomari F. *Artificial neural network model for steel–concrete bond prediction*. Engineering Structures. 2009 Aug 1; **31**(8):1724-33.
163. Mashrei MA, Seracino R, Rahman MS. *Application of artificial neural networks to predict the bond strength of FRP-to-concrete joints*. Construction and Building Materials. 2013 Mar 1; **40**:812-21.
164. Cevik A, Guzelbey IH. *Neural network modeling of strength enhancement for CFRP confined concrete cylinders*. Building and Environment. 2008 May 1; **43**(5):751-63.
165. Cevik A, Guzelbey IH. *Neural network modeling of strength enhancement for CFRP confined concrete cylinders*. Building and Environment. 2008 May 1; **43**(5):751-63.
166. Jalal M, Ramezani-pour AA. *Strength enhancement modeling of concrete cylinders confined with CFRP composites using artificial neural networks*. Composites Part B: Engineering. 2012 Dec 1; **43**(8):2990-3000.
167. Dai J, Ueda T, Sato Y. *Development of the nonlinear bond stress–slip model of fiber reinforced plastics sheet–concrete interfaces with a simple method*. Journal of composites for construction. 2005 Feb; **9**(1):52-62.
168. Real T, Zamorano C, Ribes F, Real JI. *Train-induced vibration prediction in tunnels using 2D and 3D FEM models in time domain*. Tunnelling and Underground Space Technology. 2015 Jun 1; **49**:376-83.
169. Kulkarni M, Carnahan D, Kulkarni K, Qian D, Abot JL. *Elastic response of a carbon nanotube fiber reinforced polymeric composite: a numerical and experimental study*. Composites Part B: Engineering. 2010 Jul 1; **41**(5):414-21.
170. Raghupathy AP, Ghia U, Ghia K, Maltz W. *Boundary-condition-independent reduced-order modeling of complex 2D objects by POD-Galerkin methodology*. In 2009 25th Annual IEEE Semiconductor Thermal Measurement and Management Symposium 2009 Mar 15 (pp. 208-215). IEEE.
171. Pugasap K, Kim W, Laman JA. *Long-term response prediction of integral abutment bridges*. Journal of Bridge Engineering. 2009 Mar; **14**(2):129-39.
172. Pak A, Abdullah A. *Correct prediction of the vibration behavior of a high power ultrasonic transducer by FEM simulation*. In 2007 International Conference on Power Engineering, Energy and Electrical Drives 2007 Apr 12 (pp. 522-528). IEEE.
173. Wang E, Nelson T. *Structural dynamic capabilities of ANSYS*. In ANSYS 2002 Conference, Pittsburg, Pennsylvania, USA 2002 Apr 22.
174. ANSYS User's Manual version 14.0, ANSYS Inc., Canonsburg, PA, USA.
175. Zeidan BA. *Seismic Analysis of Dam-Reservoir-Foundation Interaction for Concrete Gravity Dams*. In International Symposium on Dams In A Global Environmental Challenges, ICOLD 2014 Jun 1.
176. Quevedo FP, Schmitz RJ, Morsch IB, Campos Filho A, BERNAUD D. *Customization of a software of finite elements to analysis of concrete*

- structures: long-term effects*. Revista IBRACON de Estruturas e Materiais. 2018 Aug; **11**(4):696-718.
177. Hokeš F, Kala J, Hušek M, Král P. *Parameter identification for a multivariable nonlinear constitutive model inside ANSYS workbench*. Procedia engineering. 2016 Jan 1; 161:892-7.
  178. Makarova NV, Polonik MV, Mantsybora AA. *Abrasive wear of Cemented Granular Composites: Experiments and Numerical Simulations*. In IOP Conference Series: Materials Science and Engineering 2018 Dec (Vol. **463**, No. 3, p. 032002). IOP Publishing.
  179. Barbero EJ, Cosso FA, Martinez X. *Identification of fracture toughness for discrete damage mechanics analysis of glass-epoxy laminates*. Applied composite materials. 2014 Aug 1; **21**(4):633-50.
  180. Massabò R, Ustinov K, Barbieri L, Berggreen C. *Fracture mechanics solutions for interfacial cracks between compressible thin layers and substrates*. Coatings. 2019 Mar; **9**(3):152.
  181. Shahbazi M. *Determination of Material Parameters of E-Glass Epoxy Laminated Composites in ANSYS*. 2016.
  182. Desayi P, Krishnan S. *Equation for the stress-strain curve of concrete*. In Journal Proceedings 1964 Mar 1 (Vol. **61**, No. 3, pp. 345-350).
  183. Husain HM, Al-Sherrawi MH, Ibrahim AT. *Analysis of Double Skin Composite Slabs*. Journal of Engineering. 2018; **24**(3):135-51.
  184. Sayed AM, Wang X, Wu Z. *Finite element modeling of the shear capacity of RC beams strengthened with FRP sheets by considering different failure modes*. Construction and Building Materials. 2014 May 30; **59**:169-79.
  185. Haghani R. *Analysis of adhesive joints used to bond FRP laminates to steel members—A numerical and experimental study*. Construction and building materials. 2010 Nov 1; **24**(11):2243-51.
  186. Kumar BK, Kishore LT. *Low velocity impact analysis of laminated FRP composites*. International Journal of Engineering Science and Technology. 2012; **4**(1):115-25.
  187. Pawłowski D, Szumigala M. *Flexural behavior of full-scale basalt FRP RC beams—experimental and numerical studies*. Procedia Engineering. 2015 Jan 1; **108**:518-25.
  188. Lau KT, Dutta PK, Zhou LM, Hui D. *Mechanics of bonds in an FRP bonded concrete beam*. Composites Part B: Engineering. 2001 Sep 1; **32**(6):491-502.
  189. Naya F, Herráez M, Lopes CS, González C, Van der Veen S, Pons F. *Computational micromechanics of fiber kinking in unidirectional FRP under different environmental conditions*. Composites Science and Technology. 2017 May 26; 144:26-35.
  190. Nam JW, Kim HJ, Kim SB, Jay Kim JH, Byun KJ. *Analytical study of finite element models for FRP retrofitted concrete structure under blast loads*. International Journal of Damage Mechanics. 2009 Jul; **18**(5):461-90.

191. Kachlakev DI, McCurry Jr D. *Simulated full scale testing of reinforced concrete beams strengthened with FRP composites: experimental results and design model verification*. Oregon Department of Transportation, Salem, Oregon. 2000 Jun.
192. Barbero EJ, Cosso FA, Martinez X. *Identification of fracture toughness for discrete damage mechanics analysis of glass-epoxy laminates*. Applied composite materials. 2014 Aug 1; **21**(4):633-50.
193. Massabò R, Ustinov K, Barbieri L, Berggreen C. *Fracture Mechanics Solutions for Interfacial Cracks between Compressible Thin Layers and Substrates*. Coatings. 2019 Mar; **9**(3):152.
194. Shahbazi M. *Determination of Material Parameters of E-Glass/Epoxy Laminated Composites in ANSYS*. West Virginia University; 2016.
195. Zhao X, Li H, Chen T, Cao BA, Li X. *Mechanical Properties of Aluminum Alloys under Low-Cycle Fatigue Loading*. Materials. 2019 Jan; **12**(13):2064.
196. DeMarco JP. *Mechanical Characterization And Numerical Simulation Of A Light-weight Aluminum A359 Metal-matrix Composite*. 2011.
197. Junior FS, Venturini WS. *Damage modelling of reinforced concrete beams*. Advances in Engineering Software. 2007 Aug 1; **38**(8-9):538-46.
198. Thirumump M, Kalita K, Ramachandran M, Ghadai R. *A numerical study of SCF convergence using ANSYS*. ARPN Journal of Engineering and Applied Sciences. 2015; **10**(5).
199. Ramanan L. *Simulation of non-linear analysis in ANSYS*. In ANSYS India users conference 2006.
200. Ray Browell, Guoyo Lin, *The Power of Nonlinear Materials Capability, Part 1 and 2 on modeling materials with nonlinear characteristics*. ANSYS Solutions, 2000, Canonsburg, PA.
201. Arriaga A, Lazkano JM, Pagaldai R, Zaldua AM, Hernandez R, Atxurra R, Chrysostomou A. *Finite-element analysis of quasi-static characterisation tests in thermoplastic materials: Experimental and numerical analysis results correlation with ANSYS*. Polymer testing. 2007 May 1; **26**(3):284-305.
202. Arriaga A, Pagaldai R, Zaldua AM, Chrysostomou A, O'Brien M. *Impact testing and simulation of a polypropylene component. Correlation with strain rate sensitive constitutive models in ANSYS and LS-DYNA*. Polymer Testing. 2010 Apr 1; **29**(2):170-80.
203. CEB-FIP MC. *Model code for concrete structures*. Bulletin D'Information. 1990.
204. ASTM A1034 / A1034M-10a (2015), *Standard Test Methods for Testing Mechanical Splices for Steel Reinforcing Bars*, ASTM International, 2015, West Conshohocken, PA, American Society for Testing and Materials.